

Substitution effect on the superconductivity in $Mo_{3-x}Re_xAl_2C$ with β-Mn structure prepared by microwave method

Jun-Nan Sun(孙俊男), Bin-Bin Ruan(阮彬彬), Meng-Hu Zhou(周孟虎), Yin Chen(陈银), Qing-Song Yang(杨清松), Lei Shan(单磊), Ming-Wei Ma(马明伟), Gen-Fu Chen(陈根富), and Zhi-An Ren(任治安)

Citation: Chin. Phys. B, 2021, 30 (**7**): 077401. DOI: 10.1088/1674-1056/abfb5a
Journal homepage: http://cpb.iphy.ac.cn; http://iopscience.iop.org/cpb

What follows is a list of articles you may be interested in

Superconductivity in an intermetallic oxide $Hf_3Pt_4Ge_2O$

Chengchao Xu(徐程超), Hong Wang(王鸿), Huanfang Tian(田焕芳), Youguo Shi(石友国), Zi-An Li(李子安), Ruijuan Xiao(肖睿娟), Honglong Shi(施洪龙), Huaixin Yang(杨槐馨), and Jianqi Li(李建奇)

Chin. Phys. B, 2021, 30 (**7**): 077403. DOI: 10.1088/1674-1056/abfb53

Substitution effect on the superconductivity in $Mo_{3-x}Re_xAl_2C$ with β-Mn structure prepared by microwave method

Jun-Nan Sun(孙俊男), Bin-Bin Ruan(阮彬彬), Meng-Hu Zhou(周孟虎), Yin Chen(陈银), Qing-Song Yang(杨清松), Lei Shan(单磊), Ming-Wei Ma(马明伟), Gen-Fu Chen(陈根富), and Zhi-An Ren(任治安)

Chin. Phys. B, 2021, 30 (**7**): 077401. DOI: 10.1088/1674-1056/abfb5a

Unusual electronic structure of Dirac material $BaMnSb_2$ revealed by angle-resolved photoemission spectroscopy

Hongtao Rong(戎洪涛), Liqin Zhou(周丽琴), Junbao He(何俊宝), Chunyao Song(宋春尧), Yu Xu(徐煜), Yongqing Cai(蔡永青), Cong Li(李聪), Qingyan Wang(王庆艳), Lin Zhao(赵林), Guodong Liu(刘国东), Zuyan Xu(许祖彦), Genfu Chen(陈根富), Hongming Weng(翁红明), and Xingjiang Zhou(周兴江)

Chin. Phys. B, 2021, 30 (**6**): 067403. DOI: 10.1088/1674-1056/ac0036

Temperature and doping dependent flat-band superconductivity on the Lieb-lattice

Feng Xu(徐峰), Lei Zhang(张磊), and Li-Yun Jiang(姜立运)

Chin. Phys. B, 2021, 30 (**6**): 067401. DOI: 10.1088/1674-1056/abdea5

Nodal superconducting gap in LiFeP revealed by NMR: Contrast with LiFeAs

A F Fang(房爱芳), R Zhou(周睿), H Tukada, J Yang(杨杰), Z Deng(邓正), X C Wang(望贤成) , C Q Jin(靳常青), and Guo-Qing Zheng(郑国庆)

Chin. Phys. B, 2021, 30 (**4**): 047403. DOI: 10.1088/1674-1056/abec37

Substitution effect on the superconductivity in $Mo_{3-x}Re_xAl_2C$ with β-Mn structure prepared by microwave method*

Jun-Nan Sun(孙俊男)[1,2], Bin-Bin Ruan(阮彬彬)[2,3,†], Meng-Hu Zhou(周孟虎)[2,3], Yin Chen(陈银)[2], Qing-Song Yang(杨清松)[2,4], Lei Shan(单磊)[1], Ming-Wei Ma(马明伟)[2,3], Gen-Fu Chen(陈根富)[2,3,4], and Zhi-An Ren(任治安)[2,3,4,‡]

[1] *Key Laboratory of Structure and Functional Regulation of Hybrid Materials of Ministry of Education, Institutes of Physical Science and Information Technology, Anhui University, Hefei* 230601, *China*

[2] *Institute of Physics and Beijing National Laboratory for Condensed Matter Physics, Chinese Academy of Sciences, Beijing* 100190, *China*

[3] *Songshan Lake Materials Laboratory, Dongguan* 523808, *China*

[4] *School of Physical Sciences, University of Chinese Academy of Sciences, Beijing* 100049, *China*

(Received 5 March 2021; revised manuscript received 23 March 2021; accepted manuscript online 26 April 2021)

We report the microwave synthesis and the doping effect of $Mo_{3-x}Re_xAl_2C$ ($0 \le x \le 0.3$) superconductor. Re doping into Mo_3Al_2C results in a regular shrinkage of the lattice, marked by the linear decrease of lattice parameter a from 6.868(1) Å (for Mo_3Al_2C) to 6.846(2) Å (for $Mo_{2.7}Re_{0.3}Al_2C$). Upon Re doping, T_c of $Mo_{3-x}Re_xAl_2C$ first increases and then decreases, with the maximum $T_c = 9.14$ K at the optimal doping level of $x = 0.09$. Our report provides a convenient method to synthesize $Mo_{3-x}Re_xAl_2C$ within minutes, and also marks the first Re doping study with enhanced superconductivity on the non-centrosymmetric superconductor Mo_3Al_2C.

Keywords: $Mo_{3-x}Re_xAl_2C$, superconductivity, β-Mn structure, microwave synthesis

PACS: 74.25.–q, 74.62.Dh, 74.70.Wz, 81.20.–n **DOI:** 10.1088/1674-1056/abfb5a

1. Introduction

The crystal structure of non-centrosymmetric superconductors has the potential to realize unconventional superconductivity, and has attracted much attention in recent years.[1–3] The Cooper pair wave function of superconductor is formed by two parts: the orbit (i.e., s-, p-, or d-wave) and the spin (single or triplet) parts. In a non-centrosymmetric superconductor where space inversion symmetry is broken, the wave function could result in the mixing of spin singlet and spin triplet.[1,4] In 2004, a heavy fermion superconductor $CePt_3Si$ with a non-centrosymmetric crystal structure was reported to demonstrate intriguing physical properties, such as the extraordinarily large upper critical field and line nodes in the superconducting gap, which led to an upsurge of research on non-centrosymmetric superconductors,[5] such as $CeRh_3Si$,[6] $CeIrSi_3$,[7] UIr,[8] and $A_2Mo_3As_3$ (A = K, Rb, Cs).[9–11]

In 1963, Jeitschko *et al*. reported several compounds of the M_3Al_2C (M = Mo, Nb, Ta, V, Ti) type, and discovered a new non-centrosymmetric superconductor Mo_3Al_2C which has a β-Mn type structure.[12] Since then, a series of superconductors of the same structural family, such as Li_2Pt_3B, Cr_2Re_3B,[13] Rh_2Mo_3N,[14] Cu_2Pt_3B,[15] Al_2W_3C,[16] and Mg_2Rh_3P[17] have been discovered one after another. Among them, Mo_3Al_2C marks the highest superconducting transition temperature (T_c) ~ 9 K.

In the β-Mn type superconductors, doping has been a powerful way to modulate the structure, as well as the superconducting properties. A prominent example is the $Li_2(Pd_{1-x}Pt_x)_3B$ system with a space group of $P4_332$.[18–21] Being a conventional Bardeen–Cooper–Schrieffer (BCS) superconductor on the Li_2Pd_3B side, the system gradually transforms into a spin triplet on the Li_2Pt_3B side, together with dramatic changes in the band and gap structures.[22–27] The enhancement of spin–orbit coupling (SOC) by the substitution of 4d-Pd to the 5d-Pt plays an important role.

Despite Mo_3Al_2C has a relatively high T_c and unconventional superconductivity, and shares a quite similar geometric configuration with $Li_2(Pd_{1-x}Pt_x)_3B$, research in depth is to a large extent limited due to the difficulty of synthesis. Currently, Mo_3Al_2C synthesis methods include arc-melting method, high pressure synthesis method, hot pressing method, and spark plasma sintering (SPS) method.[18,26–28] Arc-melted samples contain many impurity phases such as Mo_2C and Mo_3Al_8. The other three methods require special equipment and are resource-consuming. As a result, the doping effect of Mo_3Al_2C has not been extensively studied. Recently, Ramachandran *et al*. reported the evolutions of lattice parameters

*Project supported by the National Key Research and Development of China (Grant Nos. 2018YFA0704200 and 2016YFA0300301), the National Natural Science Foundation of China (Grant Nos. 12074414 and 11774402), and the Strategic Priority Research Program of Chinese Academy of Sciences (Grant No. XDB25000000).

†Corresponding author. E-mail: bbruan@mail.ustc.edu.cn

‡Corresponding author. E-mail: renzhian@iphy.ac.cn

© 2021 Chinese Physical Society and IOP Publishing Ltd

and T_c for $Mo_{3-x}Nb_xAl_2C$ ($0 \leq x \leq 0.25$) and $Mo_{3-x}Ru_xAl_2C$ ($0 \leq x \leq 0.15$) systems. Their results suggested that the superconductivity in Mo_3Al_2C was quickly suppressed with increasing content of Nb and Ru.[29] In this paper, to further understand the physical properties of Mo_3Al_2C, we choose to dope Re into the Mo sites in Mo_3Al_2C. As Re possesses one more valence electron compared to Mo, it is expected to introduce electrons into the system, which may modify the band structure as well as the physical properties. Moreover, we present a convenient method to synthesize Mo_3Al_2C for the first time. By applying the microwave method,[30] polycrystalline $Mo_{3-x}Re_xAl_2C$ ($0 \leq x \leq 0.3$) samples were successfully obtained. We also report the systematic study of Re doping effect in Mo_3Al_2C for the first time. Upon Re doping, the lattice shrinks monotonously, while T_c first increases and then decreases.

2. Experiment

Molybdenum powder (99.9%), rhenium powder (99.99%), aluminum powder (99.97%), and graphite sheet (99%) were obtained from Alfa Aesar. The starting materials were mixed in the Mo/Re/Al/C molar ratio of $(3-x):x:2:1$ (the total mass of the sample was approximately 0.80 g), pressed into a pellet, and loaded into an alumina crucible (3 mL). All the above manipulations were carried out in an argon filled glove box (content of $O_2 < 0.01$ ppm). The crucible was buried in 3 g carbon black in a lager alumina crucible, and then shielded with another crucible to prevent the carbon black from splashing. The assembly was sintered in a domestic microwave oven at a power of 1000 W for 3 min. Our assembly resembled the one illustrated in Ref. [31] with some minor modifications. Likewise, the carbon black was directly contacted with air. This method is effective since the carbon black will generate a protective atmosphere at high temperature. The final products were dark grey, hard, and stable in air.

Crystal structure of the synthesized polycrystalline sample was examined at room temperature using a PAN-analytical x-ray diffractometer with Cu-K_α radiation. The magnetic properties of the samples were measured on the magnetic property measurement system (MPMS) of Quantum Design. The instrument uses a superconducting quantum interference device (SQUID) to measure the magnetic field and magnetization. The magnetic susceptibility of the samples was determined in the temperature range of 4 K to 12 K under an applied magnetic field of 10 Oe. The electrical resistivity was measured using a conventional dc four-probe method with a measuring current of 1 mA in the temperature range between 4 K and 300 K, using a physical property measurement system (PPMS, Quantum Design). The specific heat was also measured on PPMS, using a time-relaxation method between 4 K and 20 K under zero magnetic field.

3. Results and discussion

Figure 1(a) displays the powder x-ray diffraction (PXRD) patterns of the synthesized samples of $Mo_{3-x}Re_xAl_2C$ ($0 \leq x \leq 0.3$). The main diffraction peaks can be indexed with a cubic unit cell of β-Mn type Mo_3Al_2C with the space group of $P4_132$ (No. 213), and are in good agreement with the reference pattern for Mo_3Al_2C.[18,27,28] The residual minor peaks come from a small amount of impurity phase, which is identified as α-Mo_2C. According to the Rietveld refinement of each sample, there is about 10%–15% (by weight) of α-Mo_2C as the impurity. As the Re doping content increases, the lattice parameter a shrinks regularly, which is clearly evidenced by the shift of the (310) peak position toward higher 2θ values (see Fig. 1(b)). Figure 1(d) shows the evolution of lattice parameter a upon Re concentration. The lattice parameter a gradually decreases from 6.868(1) Å (for Mo_3Al_2C) to 6.846(2) Å (for $Mo_{2.7}Re_{0.3}Al_2C$), showing a linear decrease upon Re doping. This is consistent with the Vegard's law since Re has a smaller atomic radius than Mo.[33] The result indicates a successful doping of Re into the Mo sites in Mo_3Al_2C. It should be mentioned that samples with higher Re doping levels ($x > 0.3$) were also synthesized. However, impurities such as α-Mo_2C and Mo_3Al_8 became dominant phases, and the lattice parameter a for the $Mo_{3-x}Re_xAl_2C$ phase did not show a regular change. Therefore, the doping limit for $Mo_{3-x}Re_xAl_2C$ in our research was around $x = 0.3$.

It should be emphasized that the phase purity of our sample is comparable with Mo_3Al_2C made by hot pressing method and spark plasma sintering method. Yet the microwave method described here is far more convenient and resource-saving by a synthesis process within minutes.

The relationship between the resistivity and temperature of the $Mo_{3-x}Re_xAl_2C$ ($0 \leq x \leq 0.3$) sample is shown in Fig. 2. Each curve has been normalized by its value at 250 K for a clear presentation. The temperature dependence of the resistivity shows typical metallic behavior, the resistivity decreases with decreasing temperature. Nevertheless, the residual resistivity ratio (*RRR*) for each sample is small, suggesting the resistivity of $Mo_{3-x}Re_xAl_2C$ is not sensitive to temperature. It should be noted that this kind of temperature dependence of resistivity is intrinsic to Mo_3Al_2C, and is not due to the impurity or grain boundary scattering, as demonstrated in high quality, compact samples made by the SPS method.[28,29] Small values of *RRR* were also observed in the isostructural superconductor Rh_2Mo_3N[14] and Al_2W_3C,[16] implying this phenomenon might be common in the β-Mn type carbides and nitrides.

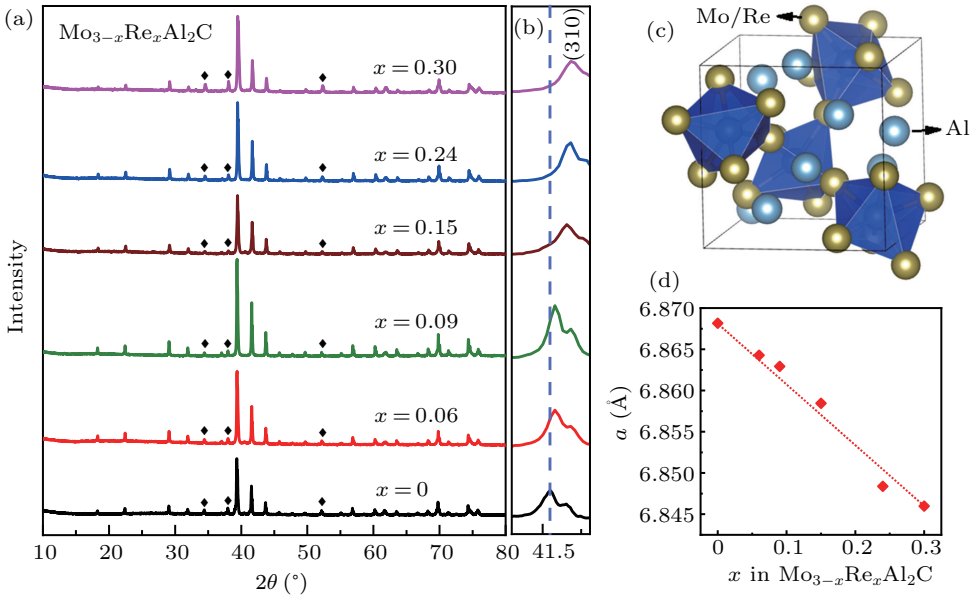


Fig. 1. (a) Powder XRD diffraction pattern of $Mo_{3-x}Re_xAl_2C$ ($0 \le x \le 0.3$), where the diamond symbol marks the Mo_2C phase. (b) Expanded view of the (310) peak in $Mo_{3-x}Re_xAl_2C$ ($0 \le x \le 0.3$). (c) Three-dimensional crystal structure of Mo_3Al_2C, produced using the VESTA software.[32] The yellow balls represent Mo/Re atoms, and the light blue balls represent Al atoms. The black line indicates a unit cell. (d) Evolution of lattice parameter a upon doping.

Resistivity for each sample shows a drop to zero at low temperature, indicating the occurrence of superconductivity. The inset of Fig. 2 is an enlarged view of the superconducting transition. We take the midpoint of the transition as the superconducting transition temperature T_c. From the figure, it can be seen that the undoped compound Mo_3Al_2C becomes superconducting below 9.00 K. Upon doping, the critical temperature T_c starts to increase with Re doping and reaches a maximum of 9.14 K at $x = 0.09$, then T_c rapidly decreases and drops below 8.41 K at $x = 0.3$.

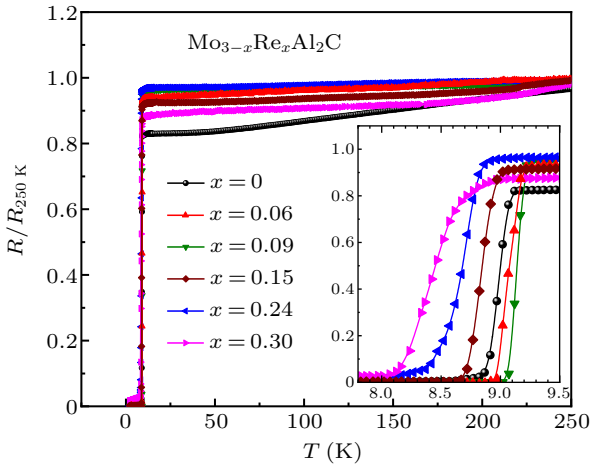


Fig. 2. Normalized resistivity of the $Mo_{3-x}Re_xAl_2C$ ($0 \le x \le 0.3$) samples changing with temperature. The inset is an enlarged view near the superconducting transitions.

Figure 3 shows the magnetic susceptibility of the $Mo_{3-x}Re_xAl_2C$ ($0 \le x \le 0.3$) doped samples under an applied magnetic field of 10 Oe. The measurements were carried out on warming after zero-field cooling (ZFC process) and then on cooling in a field (FC process). The magnetic susceptibility data exhibit marked drops, in both ZFC and FC processes, suggesting the occurrence of superconductivity. A small amount of Re doping ($x \le 0.09$) at the Mo site can improve the superconductivity of the sample. But as the doping amount further increases, the superconducting transition temperature T_c of the sample begins to decrease. For each sample, T_c obtained from the magnetic measurement is consistent with T_c from the resistivity measurement. For all these samples, the diamagnetic signals in FC curves are significantly smaller than those in the ZFC runs, indicating a strong pinning effect in $Mo_{3-x}Re_xAl_2C$. Unlike the Nb or Ru doping in Mo_3Al_2C,[29] where the superconducting volume fraction (SVF) was quickly suppressed, all the samples of $Mo_{3-x}Re_xAl_2C$ show strong diamagnetic signals, validating the bulk superconductivity.

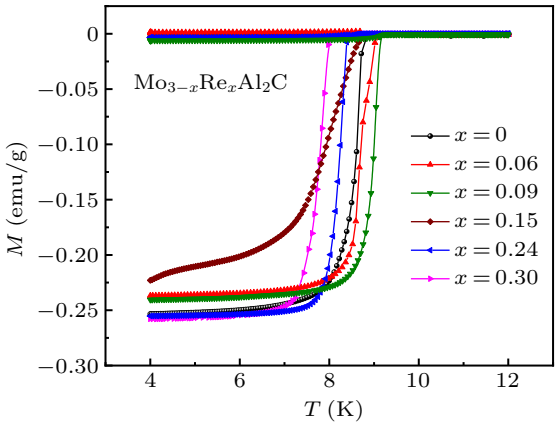


Fig. 3. Magnetic susceptibility of $Mo_{3-x}Re_xAl_2C$ ($0 \le x \le 0.3$) samples under an applied 10 Oe magnetic field.

It is worth noting that the α-Mo_2C impurity is also a superconductor. However, T_c of α-Mo_2C is not higher than 4.5 K.[34] Therefore, the impurity phase in the samples does

not affect the conclusions from the resistivity and magnetization measurements.

Figure 4(a) shows the T^2 dependence of specific heat C_p for $Mo_{3-x}Re_xAl_2C$ at $H = 0$. The normal state data can be fitted with Debye model: $C_p/T = \gamma + \beta T^2$, where γ and β are coefficients related to the electron and phonon contributions to the total specific heat, respectively.[17] Debye temperature can thus be obtained by $\Theta_D = \left(\frac{12N\pi^4R}{5\beta}\right)^{1/3}$, in which N is the number of atoms per formula, and R is the ideal gas constant. For each sample, the clear anomaly in the C_p curve indicates the superconducting transition. Accordingly, the electron–phonon coupling strength λ_{ep} can be estimated from the McMillan's relation

$$\lambda_{ep} = \frac{1.04 + \mu^* \ln(\Theta_D/1.45T_c)}{(1 - 0.62\mu^*)\ln(\Theta_D/1.45T_c) - 1.04},$$

where μ^* is the Coulomb repulsion constant. In our study, we take $\mu^* = 0.13$. We further estimate the density of states (DOS) at the Fermi level by $N(E_F) = 3\gamma/[\pi^2 k_B^2(1 + \lambda_{ep})]$.

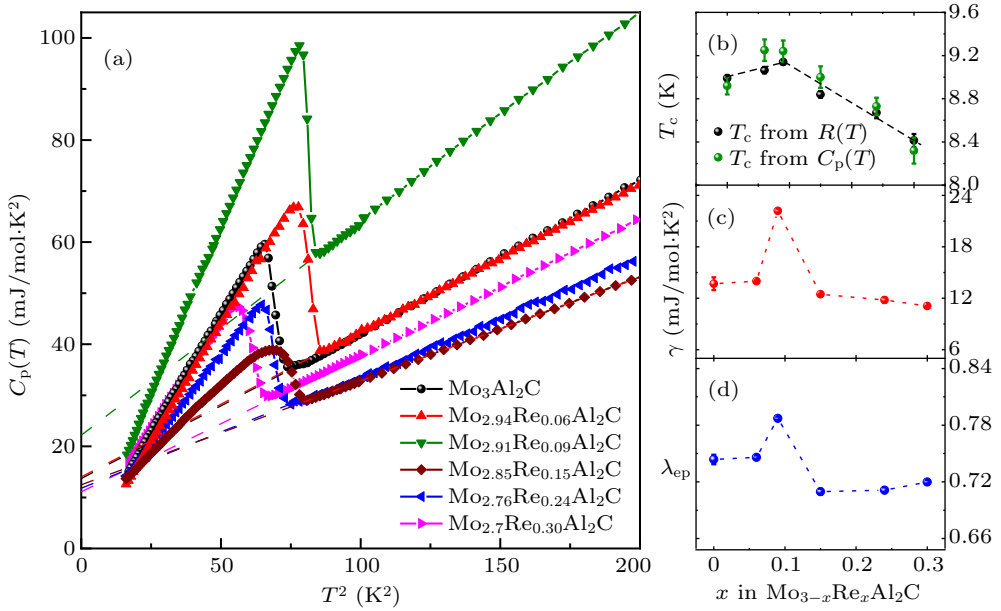


Fig. 4. (a) Low temperature heat capacity of $Mo_{3-x}Re_xAl_2C$ ($0 \le x \le 0.3$) under zero magnetic field. The normal state data is fitted with $C_p/T = \gamma + \beta T^2$, shown as the dash lines. (b)–(d) Evolution of T_c, γ, and λ_{ep} respectively upon Re doping content x. T_c is determined by both the resistivity and the specific heat measurements.

All the thermodynamic and superconducting parameters mentioned above are summarized in Table 1. Notice that the normalized specific heat changes $\Delta C_e/\gamma T_c$ of all samples are between 2.0 and 2.5 (except for the sample of $x = 0.15$, whose small $\Delta C_e/\gamma T_c$ possibly comes from the existence of non-superconducting components and/or a poor crystallization, as revealed in the broad transition in Fig. 3), and λ_{ep} is between 0.7 and 0.8. These values are comparable with those in the references,[18,27] and are well beyond the BCS weak coupling limit.

Table 1. Thermodynamic and superconducting parameters of $Mo_{3-x}Re_xAl_2C$. T_c is determined as the midpoint of the superconducting transition in the resistivity measurement.

x in $Mo_{3-x}Re_xAl_2C$	0	0.06	0.09	0.15	0.24	0.30
T_c (K)	9.00	9.06	9.14	8.84	8.67	8.41
γ (mJ·mol^{-1}·K^{-2})	13.7	14.0	22.2	12.5	11.8	11.1
Θ_D (K)	344	344	303	385	376	352
$\Delta C_e/\gamma T_c$	2.07	2.46	2.08	1.24	2.03	2.17
λ_{ep}	0.74	0.75	0.79	0.71	0.71	0.72
$N(E_F)$ (states·eV^{-1} per f.u.)	4.42	4.51	6.98	4.10	3.88	3.63

As shown in Fig. 4(a), at the superconducting state, the behavior of C_p follows a relation of $C_p \sim T^3$. As the phonon contribution of C_p is βT^3, the electronic contribution of heat capacity (C_e) also follows a power-law behavior of T^3. Although the manners of C_p at lower temperatures were not measured in our study, this kind of power-law behavior is consistent with that of the previously reported Mo_3Al_2C samples.[18,27] Our results reveal that there might be point nodes at the superconducting gap. However, since there are considerable amounts of α-Mo_2C impurity and the measuring temperature is not low enough, we are not able to draw a conclusion on the gap symmetry with merely the C_p results. Further studies on single crystals are needed to answer this question.

Figure 4(b) summarizes the change of T_c (determined by both the resistivity measurements and the specific heat measurements) of Mo_3Al_2C upon Re doping. T_c is enhanced by a small amount of Re doping before it decreases, reaching a maximum when the Re doping concentration is about 3%.

The trends of γ and λ_{ep} correspond well with the changing of T_c, as illustrated in Figs. 4(c) and 4(d). Most surprisingly, the γ of $Mo_{2.91}Re_{0.09}Al_2C$ is significantly larger than that of the other samples, indicating a much larger $N(E_F)$ ($\sim$ 150% of

the undoped sample). According to McMillan's relation, λ_{ep} is positively correlated with $N(E_F)$. Therefore, the enhancement of $N(E_F)$ should be responsible for the increase of T_c. The dramatic increase in $N(E_F)$ with such a small amount of Re doping is possibly due to the modification of Fermi surface upon electron doping introduced by Re. In this respect, a detailed study of band structure calculation of $Mo_{3-x}Re_xAl_2C$ ($0 \leq x \leq 0.3$) is definitely of interest.

4. Conclusion

In summary, we successfully prepared Mo_3Al_2C, as well as the Re-doped samples $Mo_{3-x}Re_xAl_2C$ ($0 \leq x \leq 0.3$) by a microwave method for the first time. We systematically studied the crystal structure and the basic superconducting parameters. With the increase of Re content x, the lattice parameter a decreases linearly, while T_c is enhanced by a small amount of Re doping up to $x = 0.09$ before it decreases. The increase of T_c is possibly due to the enhancement of $N(E_F)$, which may result from the modification of band structure upon electron doping. Our results not only provide a new convenient way to produce Mo_3Al_2C within minutes, they also shed lights on the study of the unconventional superconducting mechanism in Mo_3Al_2C.

References

[1] Smidman M, Salamon M B, Yuan H Q and Agterberg D F 2017 *Rep. Prog. Phys.* **80** 036501

[2] Yoshida H, Okabe H, Matsushita Y, Isobe M and Takayama-Muromachi E 2017 *Phys. Rev. B* **95** 184514

[3] Kneidinger F, Bauer E, Zeiringer I, Rogl P, Blaas-Schenner C, Reith D and Podloucky R 2015 *Physica C* **514** 388

[4] Gor'kov L P and Rashba E I 2001 *Phys. Rev. Lett.* **87** 037004

[5] Bauer E, Hilscher G, Michor H, Paul C, Scheidt E W, Gribanov A, Seropegin Y, Noel H, Sigrist M and Rogl P 2004 *Phys. Rev. Lett.* **92** 027003

[6] Kimura N, Ito K, Saitoh K, Umeda Y, Aoki H and Terashima T 2005 *Phys. Rev. Lett.* **95** 247004

[7] Sugitani I, Okuda Y, Shishido H, Yamada T, Thamizhavel A, Yamamoto E, D. Matsuda T, Haga Y, Takeuchi T, Settai R and Ōnuki Y 2006 *J. Phys. Soc. Jpn.* **75** 043703

[8] Akazawa T, Hidaka H, Fujiwara T, Kobayashi T C, Yamamoto E, Haga Y, Settai R and Nuki Y 2004 *J. Phys.: Condens. Matter* **16** L29

[9] Mu Q G, Ruan B B, Zhao K, Pan B J, Liu T, Shan L, Chen G F and Ren Z A 2018 *Sci. Bull.* **63** 952

[10] Zhao K, Mu Q G, Ruan B B, Zhou M H, Yang Q S, Liu T, Pan B J, Zhang S, Chen G F and Ren Z A 2020 *Chin. Phys. Lett.* **37** 097401

[11] Zhao K, Mu Q G, Ruan B B, Liu T, Pan B J, Zhou M H, Zhang S, Chen G F and Ren Z A 2020 *APL Mater.* **8** 031103

[12] Johnston J, Toth L, Kennedy K and Parker E R 1964 *Solid State Commun.* **2** 123

[13] Niimura H, Kawashima K, Inoue K, Yoshikawa M and Akimitsu J 2014 *J. Phys. Soc. Jpn.* **83** 044702

[14] Wei W, Zhao G. J, Kim D. R, Jin C, Zhang J. L, Ling L, Zhang L, Du H, Chen T. Y, Zang J, Tian M, Chien C L and Zhang Y 2016 *Phys. Rev. B* **94** 104503

[15] Salamakha L P, Sologub O, Stöger B, Michor H, Bauer E and Rogl P F 2015 *J. Solid State Chem.* **229** 303

[16] Ying T P, Qi Y P and Hosono H 2019 *Phys. Rev. B* **100** 094522

[17] Iyo A, Hase I, Fujihisa H, Gotoh Y, Takeshita N, Ishida S, Ninomiya H, Yoshida Y, Eisaki H and Kawashima K 2019 *Phys. Rev. Mater.* **3** 124802

[18] Bauer E, Rogl G, Chen X Q, Khan R T, Michor H, Hilscher G, Royanian E, Kumagai K, Li D. Z, Li Y Y, Podloucky R and Rogl P 2010 *Phys. Rev. B* **82** 064511

[19] Togano K, Badica P, Nakamori Y, Orimo S, Takeya H and Hirata K 2004 *Phys. Rev. Lett.* **93** 247004

[20] Badica P, Kondo T and Togano K 2005 *J. Phys. Soc. Jpn.* **74** 1014

[21] Takeya H, Hirata K, Yamaura K, Togano K, El Massalami M, Rapp R, Chaves F A and Ouladdiaf B 2005 *Phys. Rev. B* **72** 104506

[22] Yuan H Q, Agterberg D F, Hayashi N, Badica P, Vandervelde D, Togano K, Sigrist M and Salamon M B 2006 *Phys. Rev. Lett.* **97** 017006

[23] Nishiyama M, Inada Y and Zheng G Q 2007 *Phys. Rev. Lett.* **98** 047002

[24] Badica P, Salem-Sugui S, Alvarenga A D and Jakob G 2010 *Supercond. Sci. Technol.* **23** 105018

[25] Peets D C, Eguchi G, Kriener M, Harada S, Shamsuzzaman S K M, Inada Y, Zheng G Q and Maeno Y 2012 *J. Phys.: Conf. Ser.* **400** 022096

[26] Sekine C, Sai U, Hayashi J, Kawamura Y and Bauer E 2017 *J. Phys.: Conf. Ser.* **950** 042028

[27] Karki A B, Xiong Y M, Vekhter I, Browne D, Adams P W, Young D P, Thomas K R, Chan J Y, Kim H and Prozorov R 2010 *Phys. Rev. B* **82** 064512

[28] Koyama T, Maeda Y, Yamazaki T, Ueda K I, Mito T, Kohara T, Waki T, Tabata Y, Tsunemi H, Ito M and Nakamura H 2013 *J. Phys. Soc. Jpn.* **82** 073709

[29] Ramachandran B, Jhiang J Y, Kuo Y K, Kuo C N and Lue C S 2016 *Supercond. Sci. Technol.* **29** 035003

[30] Pan B J, Zhao K, Liu T, Ruan B B, Zhang S, Chen G F and Ren Z A 2019 *Chin. Phys. Lett.* **36** 017401

[31] Murgia F, Antitomaso P, Stievano L, Monconduit L and Berthelot R 2016 *J. Solid State Chem.* **242** 151

[32] Momma K and Izumi F 2008 *J. Appl. Crystallogr.* **41** 653

[33] Tarutani Y and Kudo M 1977 *J. Less-Common Met.* **55** 221

[34] Athanasiou N S 1997 *Mod. Phys. Lett. B* **11** 939